

# Stabilizing Highly Loaded Silicon Nitride Aqueous Suspensions Using Comb Polymer Concrete Superplasticizers

Lisa M. Rueschhoff, Jeffrey P. Youngblood, and Rodney W. Trice<sup>†</sup>

School of Materials Engineering, Purdue University, West Lafayette, Indiana 47907

The stabilization of highly loaded silicon nitride suspensions will afford the processing of complex and near-net shaped parts using methods such as injection molding or direct write additive manufacturing. In this study, aqueous silicon nitride suspensions up to 45 vol% solids loading were dispersed using commercially available comb-type copolymer. These copolymers are used as superplasticizers in the concrete industry and are referred to as water-reducing admixtures (WRAs). Four different WRA dispersants were examined and chemical analysis determined that each was made up of a sodium salt of polyacrylic acid (PAA-Na) backbone with neutral polyethylene oxide (PEO) side chains that afford steric stabilization. The general structures of the WRAs were compared to each other by measuring the relative areas of their prominent FTIR peaks and calculating a PAA-Na/PEO peak ratio. Suspensions were made with as-received silicon nitride powders with 5 wt% aluminum oxide and 5 wt% yttrium oxide added as sintering aids. Three of the four WRA dispersants studied were able to produce suspensions with 43 vol% solids loading and 5 vol% polymer dispersant, while exhibiting a yield-pseudoplastic behavior up to  $30 \text{ s}^{-1}$ . At higher solids loading (45–47 vol%), a shift to shear-thickening behavior was observed at a critical shear rate for these WRAs. Those WRAs with a lower PAA-Na/PEO peak ratio displayed better stabilization and diminished shear-thickening behavior. The vol% of the dispersant was optimized producing yield-pseudoplastic suspensions containing 45 vol% solids loading with yield stresses less than 75 Pa, no shear-thickening behavior, and viscosities less than 75 Pa·s for shear rates in the range of  $1\text{--}30 \text{ s}^{-1}$ .

## I. Introduction

SILICON nitride ( $\text{Si}_3\text{N}_4$ )-based ceramics have been the focus of research efforts that accelerated in the 1960s due to a search for new materials with good high-temperature mechanical properties and thermal shock resistance.<sup>1</sup>  $\text{Si}_3\text{N}_4$  is promising for gas turbine engine parts, as well as other numerous structural applications due to high flexural strength, fracture resistance, hardness, superior wear resistance, and substantial creep resistance up to  $1350^\circ\text{C}$ .<sup>2</sup> These beneficial properties arise from dense microstructures containing interlocking  $\beta\text{-Si}_3\text{N}_4$  acicular grains that deflect and bridge propagating cracks.<sup>3</sup> Dense  $\text{Si}_3\text{N}_4$  parts have traditionally been made using tape casting and hot pressing, both methods which cannot form complex shapes and require multiple costly steps.<sup>4,5</sup> More complex-shaped parts have been made via processes such as gel-casting<sup>6</sup> and injection molding.<sup>7</sup> Gel-casting of  $\text{Si}_3\text{N}_4$  has been accomplished via a cross-linking reaction in slurries with solids loading upwards

of 45 vol%, with dried parts containing approximately 6 wt% polymer.<sup>6</sup> However, these parts are machined into complex shapes after forming while in their green state.<sup>6</sup> In a traditional powder injection molding (PIM) approach, a  $\text{Si}_3\text{N}_4$  feedstock containing 20 wt% of polymer mixture of paraffin wax, stearic acid, and polypropylene was used to mold parts that achieved full density after sintering.<sup>7</sup> Heating up to  $180^\circ\text{C}$  was required to soften the polymer prior to forming, which must be removed prior to handling.<sup>7</sup> Furthermore, removal of large volume of polymer during binder burnout in traditional PIM has been shown to disrupt the integrity of the formed part due to warpage and other drying defects.<sup>8</sup>

Thus, there is a need for continued development of processing methods to form dense complex-shaped parts of  $\text{Si}_3\text{N}_4$ . One approach that uses neither cross-linking gels or requires heating prior to forming is to form highly loaded aqueous silicon nitride suspensions (>40 vol%) that have low viscosities at room temperature so that they are easily flowable. These low viscosity flowable suspensions could be used in room-temperature injection molding and direct ink writing, both methods of which have been successful in forming different ceramic systems.<sup>9–11</sup> In order to achieve low viscosities, the system must be stabilized to reduce particle attractions and subsequent flocculation, which becomes a difficult step in  $\text{Si}_3\text{N}_4$  due to the complex surface and solution chemistry of the system.

As-received silicon nitride powders contain a layer of silica on the surface less than a nanometer in thickness,<sup>12</sup> which aid in the liquid-phase sintering processes by forming a silicate glass that is modified by ceramic powders added as sintering aids (such as yttria, alumina, and other rare-earth oxides).<sup>13</sup> The surface silica contains silanol ( $\text{Si-OH}$ ) and secondary amine ( $\text{Si}_2\text{-NH}$ ) groups that can leach over time in an aqueous environment, altering the surface chemistry of the powders of the solution.<sup>14</sup> The amount of surface dissolution depends on the physical and chemical properties of the starting ceramic powder, as well as its manufacturing and processing history.<sup>15</sup> Other research on producing aqueous silicon nitride suspensions has utilized calcination steps to form a thicker silica layer, and therefore more silanol surface groups, on the surface of the silicon nitride particles.<sup>16,17</sup> While the increase of these silanol groups increase the particle's negative potential causing repulsion between particles,<sup>18</sup> the increase in silica leads to less desirable high-temperature mechanical properties of sintered bodies since they contain more intergranular silica glass.<sup>19</sup> Another method to stabilize ceramic powders has been through traditional charged polyelectrolyte dispersants consisting of low-molecular weight water-soluble polymers that rely on electrostatic charge repulsion to stabilize powders.<sup>20,21</sup> However, electrostatic stabilization is often not enough to stabilize powder systems with complex surface and solution chemistry such as silicon nitride.<sup>22</sup> In this case, steric stabilization is required to form a more stable suspension at high solids loading<sup>22</sup> without changing the surface chemistry and therefore the properties of final sintered parts.

The concrete research field has been a pioneer in developing water-soluble polymer dispersants for optimum steric

R. Bordia—contributing editor

Manuscript No. 38180. Received February 11, 2016; approved July 5, 2016.

<sup>†</sup>Author to whom correspondence should be addressed. e-mail: rtrice@purdue.edu

hindrance. A concrete mixture is a prime example of complex surface and solution chemistry as the variation in particles and ions in solution that result from hydration reactions make the stability of the system complicated.<sup>23–25</sup> Superplasticizers that are used in the concrete industry to reduce the amount of water needed in a mixture (due to more stabilized suspensions) are deemed high-range water-reducing admixtures (WRAs). The first generation of WRAs consisted of linear polyelectrolytes such as sulfonated naphthalene formaldehyde and polyacrylic acid (PAA), both of which have one ionizable group per monomer.<sup>23</sup> The second generation of WRAs achieve much larger stability over longer time scales and consist of copolymers with a comb structure with either PAA or polymethylmethacrylate backbone and charge neutral polyethylene oxide (PEO) teeth grafted to the backbone at frequent intervals.<sup>22,23</sup> These polymers have been found to offer stability in concrete systems through adsorption of the charged backbone to the cement particle surfaces, while the PEO side chains extend into the solution to offer steric stabilization.<sup>26</sup>

It has been found that similar comb-type copolymers consisting of an anionic backbone and uncharged PEO side chains offer colloidal stability via steric stabilization to ceramic powder systems with complex surface and solution chemistry.<sup>22,27</sup> Whitby et al. found a PAA/PEO comb polymer effective in stabilizing silica suspensions,<sup>27</sup> and since the  $\text{Si}_3\text{N}_4$  particles have a layer of silica on the surface, it is hypothesized that a similar PAA/PEO comb polymer could also be useful in stabilizing the ceramic system. In fact, Laarz and Bergstrom compared commercial polymethacrylic acid (PMAA) comb polymers with PEO side chains (one with a sodium salt and one with ammonium salt backbone PMAA polymer) to a benchmark ammonium salt of PAA dispersant to stabilize 20 vol%  $\text{Si}_3\text{N}_4$  suspensions and reported what they called a “minor influence on the colloidal stability” with the comb polymer.<sup>28</sup> Their only minor increase in stability could be due to their low solids loading and therefore more simplified particle interactions and less ions in solution due to disassociation, or the backbone could be less effective, as compared to the PAA backbone, at adsorbing onto the ceramic particle surfaces.

This work aims to use commercially available WRAs to achieve high solids loading of  $\text{Si}_3\text{N}_4$  powders. Figure 1 illustrates the general structure of the comb polymers that will be studied, and their theorized mechanism of adsorption on the silicon nitride surface to impart steric stabilization via PEO teeth that extend into the solution. Using commercially available polymers will avoid the complex grafting of comb-type copolymers as used in previous work. The goal of the study is to optimize the aqueous suspensions made with  $\text{Si}_3\text{N}_4$  powders with no calcination pretreatments and at high solids loadings, both of which will allow for the future production of parts with the highest sintered densities and mechanical properties. Optimizing rheology and particle stabilization at solids loadings greater than 43 vol% will also afford the investigation of the most challenging stabilization scenario containing a system with a large amount of particle

interactions and a large magnitude of ions in solution due to dissociation.

## II. Experimental Approach

### (1) Materials and Suspension Preparation

Alpha silicon nitride powders (SNE-10; UBE Industries, Tokyo, Japan), with company specified  $d_{50}$  of 0.50  $\mu\text{m}$  and specific surface area (SSA) of 9–13  $\text{m}^2/\text{g}$ , were used in this study. Powders from lot number A136828 were used with company specified SSA of 10.6  $\text{m}^2/\text{g}$ . It has been found in a study by Okada et al. on SNE-10 powders that the oxide layer present in the surface is approximately 0.5 nm, as determined using X-ray Auger electron spectroscopy.<sup>12</sup> All experiments utilized 5 wt% aluminum oxide ( $\text{Al}_2\text{O}_3$ ) with an average particle size of 0.50  $\mu\text{m}$  and SSA of 7 to 12  $\text{m}^2/\text{g}$  (A-16 SG; Almatix, Leetsdale, PA) and 5 wt% yttrium oxide (Sigma Aldrich, St. Louis, MO) with a company specified  $d_{50}$  of 2–10  $\mu\text{m}$  as sintering aids. While this study does not specifically focus on the sintering of silicon nitride parts, the goal was to optimize solids loading and rheology with sintering aids so that sintering studies can be done in the future. The sintering aids were mixed with  $\text{Si}_3\text{N}_4$  powders, without milling media, using a dual-centrifugal speed mixer (DAC 400, Flacktek Inc, Landrum, SC) for 2 min at 850 rpm to ensure uniformity.

The commercially available concrete WRAs used in this study come as aqueous solution and were ADVA 190 and ADVA CAST 575 (W.R. Grace, Columbia, MD) and Glenium 3030 NS and Glenium 7500 (BASF, Ludwigshafen, Germany) and will henceforth be referred to as dispersants. Reference samples of PEO (Sigma Aldrich) and a sodium salt of PAA (PAA-Na, Polysciences, Warrington, PA) were used as standards in some characterization experiments discussed in following sections.

Silicon nitride suspensions were fabricated by mixing reverse osmosis (RO) water with the appropriate dispersant content, followed by slowly mixing in as-received silicon nitride and sintering aid powder mixture. The previously mentioned dual-centrifugal mixer was used to thoroughly mix these highly loaded suspensions. Mixing increments were done for 1–3 min starting at 800 rpm and increasing to up to 1500 rpm with increasing solids loading.

### (2) Superplasticizer Dispersant Characterization

Commercially available WRAs were characterized in order to differentiate and understand their performance as dispersants in the  $\text{Si}_3\text{N}_4$  system. A qualitative comparison of the relative concentration of the components in each WRA dispersant was determined using a Spectrum 100 FTIR (Perkin Elmer, Waltham, MA) in Attenuated Total Internal Reflectance mode using a germanium crystal. The dispersants, as well as reference PEO (35 000 g/mol) and PAA-Na (3000 g/mol) samples, were casted on a glass slide and after evaporation were dried in a vacuum desiccator under high vacuum overnight. For each sample, four scans were taken from 650 to

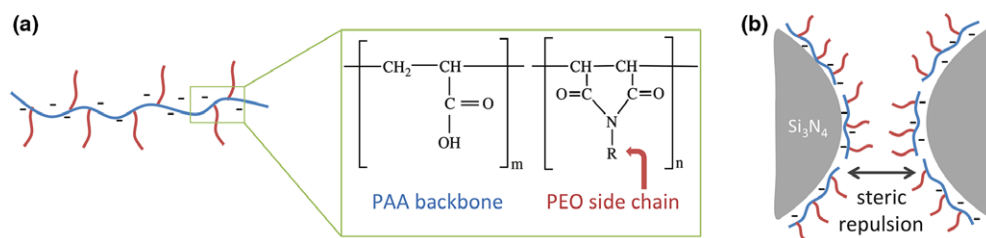


**Fig. 1.** Schematic illustration of (a) molecular structure of typical comb polymer water-reducing admixtures composed of PAA backbones with PEO side chains ( $\text{R} = (\text{CH}_2\text{CH}_2\text{O})_x\text{-CH}_3$ ) and (b) coating of  $\text{Si}_3\text{N}_4$  particles with charged PAA backbone and PEO side chains providing steric repulsion between particles to stabilize the suspension (not drawn to scale).

4000 nm wavelengths. Peak areas in scans for the dispersant samples were compared to peaks for the reference PEO and PAA-Na samples to determine the relative amounts of each in the dispersants. Gel permeation chromatography (GPC) was used to determine relative sizes of the comb polymer dispersants. Measurements were performed using a Malvern Viscotek GPCmax instrument with refractive index and dual light scattering detectors. Test solutions were made with 5 mg/mL active polymer dispersant in a phosphate-buffered saline solution and were analyzed at a flow rate of 1 mL/min.

Thermogravimetric analysis (TA Instruments, Newcastle, DE) was used to determine the burnout temperature and relative water content of the as-received dispersants. Using a flowing nitrogen atmosphere, approximately 20 mg of each dispersant was heated at 10°C/min in an alumina crucible. The water content in each dispersant was quantified by measuring the weight loss upon heating from 25°C through the plateau in mass loss. Mass loss typically started at 100°C and continued through 400°C. Note that the amount of dispersant added accounted for the water content; thus, it was constant throughout this study. Further heating of the sample started the process of binder burnout. The binder burnout temperature was determined as the temperature at which the weight loss reached a minimum plateau.

The zeta potential of the as-received ceramic powders in solutions of RO water with and without dispersant was determined using a ZetaSizer Nano Z (Malvern Instruments, UK). Each zeta potential sample was taken from a stock solution of RO water with or without 0.25 wt% dispersant mixed with 0.05 wt% silicon nitride (including sintering aids) using an ultrasonic probe (Model 250, Branson Ultrasonics, Danbury, CT) for 3 min at 30% power output. For the zeta potential measurements as a function of pH, 50 mL of the stock was split in half to add either dilute HCl or NaOH to decrease and increase the pH, respectively. The pH was measured using an Oakton pH 5 meter (Vernon Hills, IL), which was calibrated with electrolytic buffer solutions of pH 4 and 10. Each zeta potential measurement at a set pH value was an average of 50 total measurements.

### (3) Rheology

Rheological studies were used to optimize dispersant concentration and to determine maximum solid loading (above 43 vol%) in the  $Si_3N_4$  suspensions. Shear stress and viscosity data as a function of shear rate were determined using a Malvern Bohlin Gemini HR rheometer (Malvern Instruments Ltd, Worcestershire, UK) with a 25 mm cup and bob geometry fixture and a gap of 150  $\mu$ m. Approximately, 13 mL of each suspension was used for each test, and a water trap was used to prevent premature drying of the suspension during testing. Each suspension was presheared for 60 s at a shear rate of 1  $s^{-1}$  to ensure a uniform shear history. The applied shear rate was increased logarithmically from 0.005 to 30  $s^{-1}$  to measure the low-shear viscosity and shear stress of the samples. The shear rate ranges used in room-temperature injection molding and direct ink writing of similar materials in previous research were found to be 3–4  $s^{-1}$  and 19–25  $s^{-1}$ , respectively.<sup>9–11</sup>

The shear stress as a function of applied shear rate flow curves obtained for each sample were fitted to the Herschel–Bulkley model for yield-pseudoplastic fluids<sup>29</sup> which is defined as:

$$\sigma = \sigma_y + k\dot{\gamma}^n$$

where  $\sigma$  is the measured shear stress,  $\sigma_y$  is the yield stress,  $k$  is the consistency index,  $\dot{\gamma}$  is the applied shear rate, and  $n$  is the flow index (ranging from 0 to 1). A material is considered shear thinning if the flow index is less than one.<sup>30</sup> Materials

with flow index greater than one are considered dilatant (shear thickening) and are deemed undesirable for ceramic processing as they are difficult to flow and the binder can separate from the ceramic powder.<sup>31</sup> The rheological results for the suspensions were fit to this model using a method of least squares to determine the yield stress and flow index for each.

## III. Results

### (1) WRA Characterization

FTIR spectra for the four dispersants and reference polymers are shown in Fig. 2. The reference polymer spectra were used as a reference to determine the relative amounts of each (PAA-Na, PEO) in the dispersants since their chemical compositions are not disclosed. The peaks of interest, as denoted in Fig. 2, are the peak at nominally 1600  $cm^{-1}$  assigned to the carbonyl stretch (there is some shifting of the band in the dispersant spectra due to the localized chemical environment), and the peak at 1100  $cm^{-1}$  assigned to ether group stretching. These carbonyl and ether groups were the most prominent in both in the reference samples for PAA-Na and PEO, respectively, and were therefore used for the PAA-Na/PEO peak ratios. The hydroxyl peak observed near 3300  $cm^{-1}$  in the PAA-Na reference and all dispersant samples was excluded in the ratio due to the possibility of imperfect drying of the water-based dispersants, and therefore water left over in the sample could contribute to part of the peak area. The peak at approximately 2882  $cm^{-1}$  in the reference PEO and all dispersants was assigned to methylene stretching and was also excluded due to the overlap of the alkyl group peak observed at 2944  $cm^{-1}$  in the PAA-Na reference.

The PAA-Na/PEO peak ratios, as calculated from the area under the carbonyl and ether peaks in the spectra for each dispersant, are listed in Table I. Using this method, it was found that ADVA 190 had the highest ratio (0.67/1), while Glenium 7500 had the lowest (0.11/1). Since the PAA-Na exists as the backbone of the copolymer, it is assumed that a

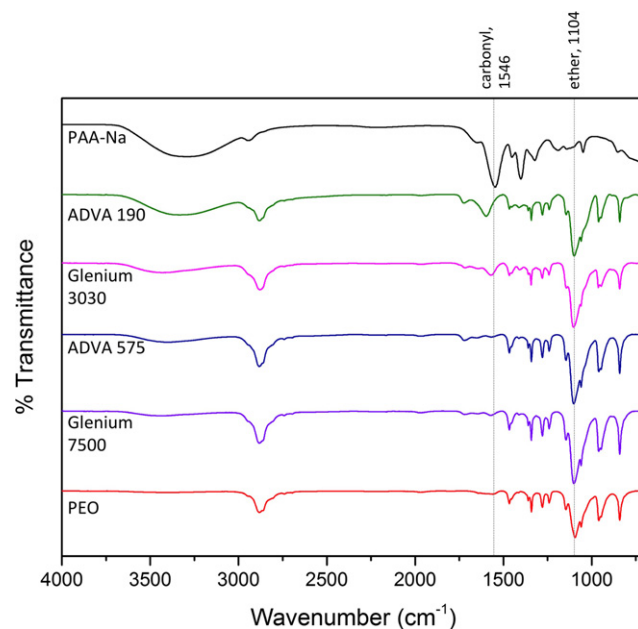


Fig. 2. FTIR spectra of the four WRAs studied along with reference spectra for PEO and a sodium salt of PAA (PAA-Na). The strong peak around 1550  $cm^{-1}$  can be attributed to the C=O (carbonyl) stretch in PAA-Na, while the peak around 1100  $cm^{-1}$  can be assigned to the C–O–C (ether) stretching hydrating bond in PEO. The ratio of the area under these peaks is used to analyze the PAA-Na/PEO peak ratio.

**Table I. Comb Polymer Dispersants Used To Stabilize Silicon Nitride Suspensions With Herschel–Bulkley Curve Fitting Parameters For Yield-Pseudoplastic Fluids**

Dispersant	PAA-Na/PEO Peak Ratio <sup>†</sup>	Sample Name	Amount of Si <sub>3</sub> N <sub>4</sub> /Y <sub>2</sub> O <sub>3</sub> /Al <sub>2</sub> O <sub>3</sub> powder (vol%)	Dispersant (vol%)	$\sigma_y$ (Pa)	$k$ (Pa·s <sup><i>n</i></sup> )	$n$
PAA-Na	1/0	PAA-Na-43-5	43	5	—	—	—
ADVA 190	0.67/1	A190-43-5	43	5	—	—	—
Glenium 3030 NS	0.27/1	G3030-43-5	43	5	22.3	11.7	0.56
		<b>G3030-45-5</b>	45	5	68.6	10.7	0.70
ADVA CAST 575	0.12/1	<b>G3030-45-6</b>	45	6	78.1	15.3	0.77
		A575-43-5	43	5	45.0	17.8	0.49
		<b>A575-45-3</b>	45	3	24.0	17.3	0.54
Glenium 7500	0.11/1	A575-45-5	45	5	54.0	50.8	0.52
		G7500-43-5	43	5	52.3	12.7	0.40
		<b>G7500-45-5</b>	45	5	54.5	11.8	0.69
PEO	0/1	G7500-47-5	47	5	167.0	27.4	0.80
		PEO-43-5	43	5	—	—	—

<sup>†</sup>Calculated via FTIR peak area ratios.

Bolded sample names refer to optimized dispersant contents at 45 vol% solid loading.

higher PAA-Na/PEO peak ratio means a lower side-chain (PEO) density and/or molecular weight compared to the other dispersants. It should be noted that this peak ratio is not meant to be quantitative, but rather is simply a qualitative estimate of relative PAA-Na/PEO content.

Gel permeation chromatography results (not shown) found the molecular weight to vary from 33 000 to 51 000 g/mol for the four dispersants. These GPC results were used only to find the relative molecular weight as this particular method is most reliable for linear polymers, and is less accurate when measuring the molecular weight of branched and more advanced structures, such as the comb polymer copolymer dispersants used here. This magnitude of molecular weight of the polymers shown here is larger than other typical ceramic dispersants used with silicon nitride such as: Darvan 821A (6000 g/mol),<sup>32</sup> Darvan C (13 000 g/mol),<sup>33</sup> and Dolapix PC33 (16 000 g/mol).<sup>17</sup> This suggests that these larger molecular weight comb polymers could have a greater steric stabilization effect due to their larger size. The magnitude of the molecular weight discovered here is consistent with reports from other research teams that found molecular weights around 20 000 g/mol of a similar concrete superplasticizer.<sup>34</sup> It has been found in a study by Laarz and Bergstrom on stabilizing Si<sub>3</sub>N<sub>4</sub> at lower solids loading (20 vol%) that PMAA-PEO grafted comb polymers effective as dispersants had molecular weights ranging from 37 200 to 43 200 g/mol.<sup>28</sup>

Figure 3 shows mass loss as a function of temperature for each of the four dispersants in a flowing nitrogen atmosphere. The water content for each dispersant is summarized in the inset of Fig. 3 and was used in calculations for suspension preparations. All four dispersants have sufficient mass loss (>97%) after approximately 420°C, indicating their feasibility as a ceramic dispersant due to their ease of burnout in a nitrogen atmosphere. The residual mass left after burnout could be due to pyrolysis products and/or sodium salt (from the backbone of the polymer) oxidation products. Experiments done on two out of the four dispersants in an oxygen flowing atmosphere (data not shown) showed an increase in the residual weight left after burnout of nominally 1%. This increase in residual weight in an oxygen atmosphere would indicate residue primarily due to oxidation products from the sodium salt backbone.

Zeta potential (in mV) as a function of pH is shown in Fig. 4. The as-received Si<sub>3</sub>N<sub>4</sub> powders in water alone show an isoelectric point (IEP) of ~5 pH, and the largest magnitude potentials are observed at ~2.5 pH and ~9 pH, of 30 and -25 mV, respectively. This matches with similar research finding an IEP of silicon nitride from 4 to 7 pH.<sup>14,28,35</sup> The IEP of Si<sub>3</sub>N<sub>4</sub> can vary greatly based on the ratio of basic

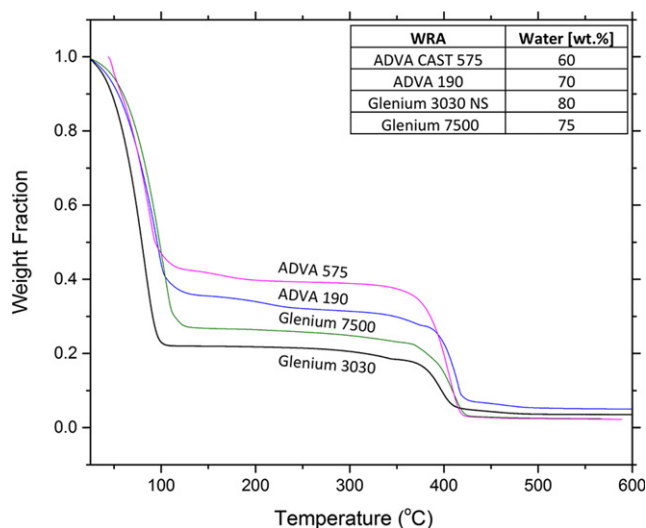


**Fig. 3.** Weight loss as a function of temperature results for dispersants as obtained via thermogravimetric analysis experiments in a flowing nitrogen atmosphere. The water content in each dispersant was quantified by measuring the weight loss upon heating from 25°C through the plateau in mass loss. Mass loss typically started at 100°C and continued through 400°C. All four samples reached >97% weight loss by approximately 420°C.

amine to acidic silanol groups present in the surface, the amounts of each varied by pretreatments of starting powders.<sup>14,17</sup> At pH values above the IEP, the powders exhibited a negative charge in water due to the formation of surface SiO<sup>-</sup> resulting from the dissociation of surface silanol groups.<sup>36</sup> The zeta potential of the as-received powders with the sintering aids added shifted the IEP to ~4 pH, with a similar shape and trend as the as-received Si<sub>3</sub>N<sub>4</sub>. The standard deviation for this data set was nominally ±7 mV and was excluded from the figure for clarity. These as-received powders mixed with sintering aids in an RO water comb polymer solution had pH values ranging from 5.39 to 6.50 and corresponding zeta potential within the standard deviation of the starting powders in water. This is consistent with other work that found no change in surface charge properties of ceramic powders with the addition of neutral polymers.<sup>37</sup> These dispersant solutions over a range of pH values showed nominally the same IEP (in the case of ADVA 575 and Glenium 7500), or slightly lower IEP values (for ADVA 190 and Glenium 3030). The powders with a reference PEO sample had a pH of 6.82 and zeta potential within the standard deviation and an IEP shift to approximately 2.7 pH, while the

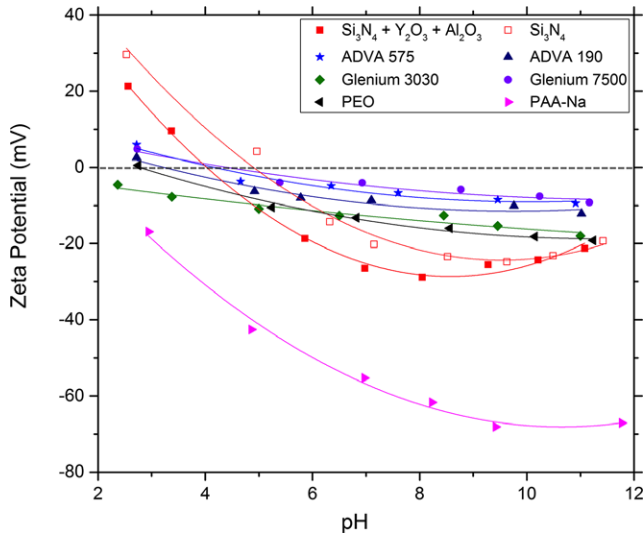


**Fig. 4.** Zeta potential of as-received  $\text{Si}_3\text{N}_4$  powder and with 5 wt%  $\text{Y}_2\text{O}_3$  and 5 wt.%  $\text{Al}_2\text{O}_3$  added as sintering aids in water and with polymer dispersants. Studies with dispersants were conducted with the sintering aid mixture. Solids loading of 0.05 wt% ceramic powder was used for all studies, with 0.025 wt% dispersant used with respect to the total mass of the sample.

reference PAA with ceramic powder had a starting pH of 9.42 corresponding to a zeta potential of  $-68$  mV (a  $\sim 3\times$  increase from the plain ceramic powder) and an IEP of less than 2 pH. The large magnitude change in zeta potential with PAA is indicative that it is adhering to the ceramic particle surface and effectively changing the surface charge,<sup>38</sup> and confirms that the PAA in the backbone of the comb polymer dispersant will adhere to the surface as well, while the PEO (which experiences no zeta potential change) provides no charge change or electrostatic repulsion. Since the dispersants themselves showed no change in zeta potential magnitude, it can be inferred that they are not contributing to any major electrostatic stabilization within the system. Any stabilization in the system is therefore likely occurring due to steric effects. This result is confirmed by reports from Yoshioka et al. who found that steric hindrance to be the dominating stabilization mechanism in concrete WRAs with PEO side chains.<sup>26</sup>

## (2) Rheology

Suspensions made with all four WRA dispersants as well as reference PAA-Na and PEO suspension are shown in Table I. Dispersant volume fractions are calculated as

amount of active polymer in the solution, excluding the water content of the WRAs. The shear stress as a function of shear rate flow curves and viscosity dependence on shear rate for suspensions made with 43 vol% solid loading and 5 vol % dispersant are shown in Figure 5. ADVA 190 as well as reference PAA-Na and PEO samples were unable to produce flowable suspensions at 43 vol% solid loading. All other samples with 43 vol% solids showed yield-pseudoplastic behavior and were fit to the Herschel–Bulkley model (correlation factor  $R^2 \sim 0.99$ ) with fitting parameters listed in Table I. Glenium 3030 had the lowest yield stress at 22.3 Pa, followed by ADVA 575 at 45.0 Pa, and Glenium 7500 at 52.3 Pa. The observed shear stress is attributed to the breaking up of flocculation in the structure,<sup>39</sup> so at this solid loading and dispersant content, it can be assumed that the addition of Glenium 3030 into the system had the greatest effect on decreasing flocs in the system. All suspensions had viscosities less than nominally 100 Pa·s in the range from 1 to 30  $\text{s}^{-1}$ , the forming range for ceramics using room-temperature injection molding and direct ink writing.<sup>9–11</sup>

Similar rheological characterization of the same suspensions with an increased solids loading to 45 vol% with dispersant content still at 5 vol%, are shown in Fig. 6, with Herschel–Bulkley fit parameters for each listed in Table I. A switch from shear-thinning (pseudoplastic) to shear-thickening (dilatant) behavior is observed at shear rates greater than 1  $\text{s}^{-1}$  for both Glenium 3030 and ADVA 575. The shear rate of the behavior switch will be referred to as the critical shear rate and is denoted in Fig. 6. At this solids loading and dispersant content, only the suspension made with Glenium 7500 exhibited solely shear-thinning behavior in the range of shear rates (0.001–30  $\text{s}^{-1}$ ) shown here. A shear-thinning to shear-thickening conversion around comparable shear rates ( $\sim 10$   $\text{s}^{-1}$ ) was observed in concrete systems using similar comb polymer dispersants.<sup>24</sup> While the precise mechanism of shear-thickening behavior is disputed for various material systems, it is known that shear-thickening behavior is nonideal for processing as it makes it difficult to form complex structures due to larger increments in energy needed to accelerate flow.<sup>25</sup> It is speculated that at this critical shear rate of conversion, the hydrodynamic forces between the particles dominate the repulsive forces which cause the particles to stick together, or cluster, temporarily.<sup>25</sup> Another order–disorder transition theory comes from Hoffman, who found that in the easily flowing state, the particles are ordered into layers, while at the critical shear rate, they shift to a disordered state, dissipating energy while flowing due to particle “jamming” which causes an increase in viscosity.<sup>40</sup> It has been found in a study on monodisperse silica powder ( $d = 0.6$   $\mu\text{m}$ ) in water that the volume fraction of the suspensions had no affect on the critical shear rate, but did affect the intensity of shear thickening (defined as the

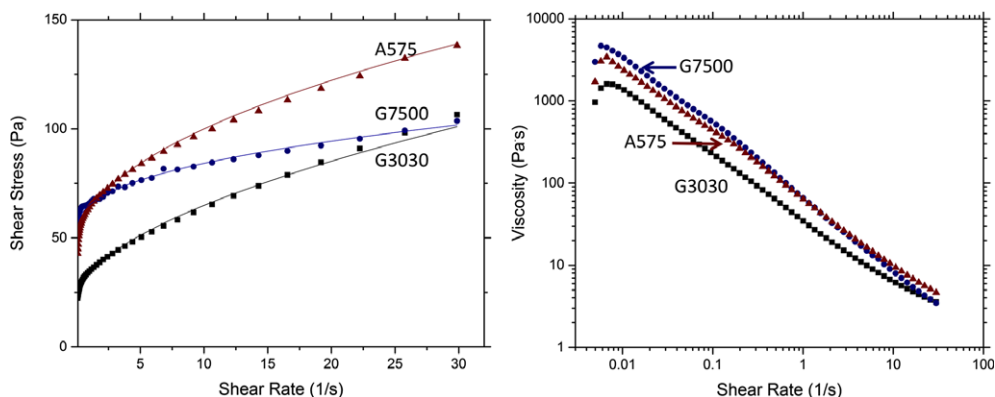


**Fig. 5.** Flow curves for silicon nitride suspensions with 43 vol% solids loading and 5 vol% dispersant content for the three studied dispersants. Curve fits to the Herschel–Bulkley fluid model are shown as solid lines with  $R^2 > 0.99$ . Viscosity as a function of shear rate shows a shear thinning trend for all three dispersants.

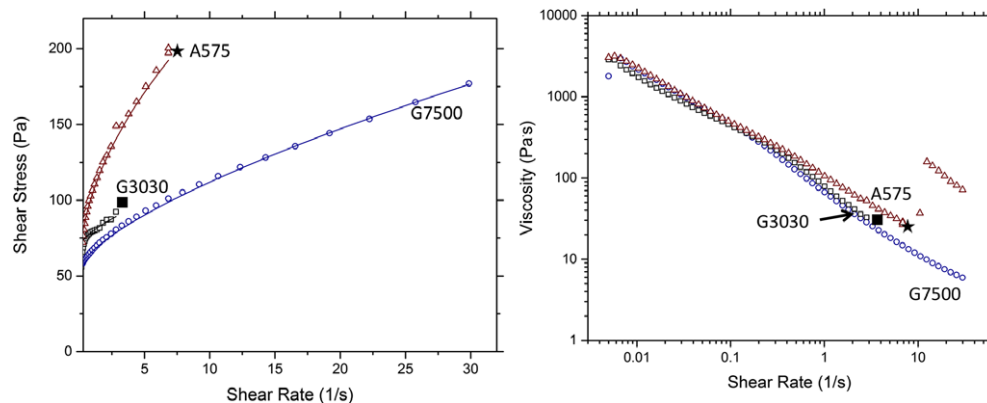


**Fig. 6.** Flow curves for silicon nitride suspensions with 45 vol% solids loading and 5 vol% dispersant content for the three studied dispersants. The shear-thickening critical shear rate is marked with (★) and (■) for ADVA 575 (A575) and Glenium 3030 (G3030), respectively. G7500 did not exhibit any shear-thickening behavior in this range of shear rates. Curve fits to the Herschel–Bulkley fluid model are shown as solid lines with  $R^2 > 0.99$ . Viscosity as a function of shear rate for the dispersants, showing a shear-thinning behavior and switch to shear-thickening behavior at the critical yield stress (data for G3030 after the critical shear rate was unable to be attained by the rheometer due to the large viscosity increase).

increase in apparent viscosity for a certain increase in shear stress).<sup>25</sup> This study did not include the use of polymer dispersants, but other studies on concrete mixtures found a critical shear rate of shear-thickening behavior only in the presence of comb polymer dispersants.<sup>24,41</sup>

Figure 7 shows a plot of the critical shear rate for 45 vol% solids loading suspensions as a function of PAA-Na to PEO peak ratio of the dispersants. A trend is observed that higher PAA-Na/PEO peak ratio dispersants experienced higher critical shear rates and would therefore be more adequate for ceramic processing. This ratio, determined via FTIR experiments outlined in Section III(1), gives an idea of backbone (PAA-Na) to side chain (PEO) make up. Dispersants with a lower ratio have either a higher density or larger molecular weight PEO side chains, which have been shown to shield the PAA backbone from ion-bridging interactions with counterions in solution in studies of similar PAA/PEO comb polymers.<sup>23</sup> This shielding of the backbone allows for better steric stabilization, and higher critical shear rate observed in this study, seen in Fig. 6. Yoshioka et al. have also found that increasing the molecular weight of PEO side chains (which would correspond to a lower PAA-Na/PEO peak ratio in this study) increases the minimum interparticle potential energy, independent of side-chain density once a minimum molecular weight is achieved.<sup>26</sup> Similarly, Kauppi

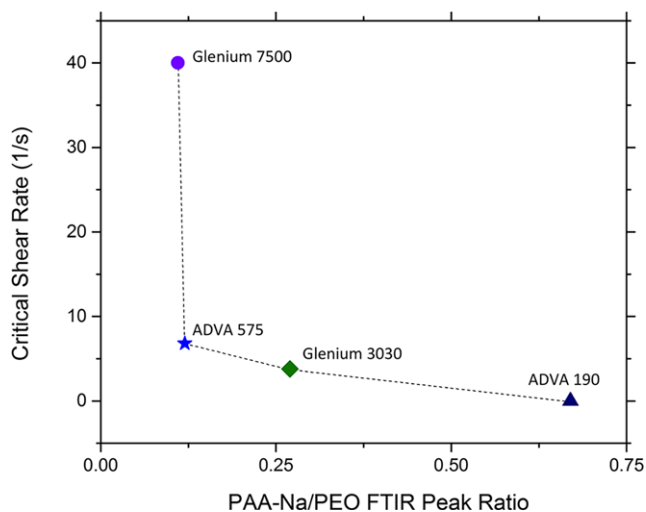


**Fig. 7.** Critical shear rate where suspensions exhibit onset of shear-thickening behavior as a function of PAA-Na/PEO peak ratio (determined via FTIR). The dotted line shown is simply to direct the eye.

et al. used atomic force microscopy to determine that commercially available comb polymers with higher molecular weight side chains had a larger conformation on the surface of magnesia powders and induce a longer range steric repulsion when compared to comb polymers with lower molecular weight side chains.<sup>21</sup> The dispersants with higher PAA-Na/PEO peak ratios have less PEO and therefore less shielding of the backbone and perform more similarly to pure PAA, which coats ceramic particles and can cause flocculation due to either counterion bridging<sup>23</sup> or bridging between particle surfaces.<sup>28</sup> PAA is also very susceptible to changes in pH, changing conformation with different ionic values, while PAA/PEO comb polymers do not experience large size changes as a result of varying pH or ionic strength, meaning the steric barrier they provide is insensitive to these variations.<sup>23</sup> This is an important consideration when dealing with  $\text{Si}_3\text{N}_4$  powder in water due to the plethora of ions in solution, coming from the dissociation of ions from the surface of the powder (as discussed in Section I). The fact that both the PAA-Na and PEO could not separately produce flowable suspensions confirms that both the backbone and side chains of the comb polymer are necessary for dispersion in this case.

In order to discover the highest critical shear rate, which will allow a wider processing range, the dispersant content at the highest solids loading for each dispersant was increased and/or decreased to find the optimum content. Figure 8 shows the viscosity as a function of shear rate for these studies. Both Glenium 3030 and ADVA 575 were studied at 45 vol% solids loading, while Glenium 7500 was studied at 47 vol% since there was no critical shear rate observed for the 45 vol% suspensions under  $30 \text{ s}^{-1}$ . Glenium 3030 experienced the highest critical shear rate, and therefore the best processing ability, at  $10 \text{ s}^{-1}$  when 6 vol% dispersant was used, corresponding to a comb polymer concentration of  $4.0 \text{ mg/m}^2$ . The ADVA 575 suspension made with 3 vol% dispersant ( $1.9 \text{ mg/m}^2$ ) experienced no shear thickening in the explored shear rate range and so was considered the most ideal at this solids loading. The suspension made with Glenium 7500 had an optimum dispersant content at 5 vol% ( $2.9 \text{ mg/m}^2$ ) corresponding to the greatest critical shear rate of approximately  $3 \text{ s}^{-1}$ . Additionally, a general increase in viscosity with increasing polymer content was observed for most samples. This has been previously attributed to dissociation of the free polymer functional group with the release of cations which impart electrostatic screening effects and result in weak flocculation of the suspension.<sup>28</sup> In some cases, a lower amount of polymer (e.g., when ADVA 575 was decreased from 3 to 2 vol%) had a higher viscosity, which is

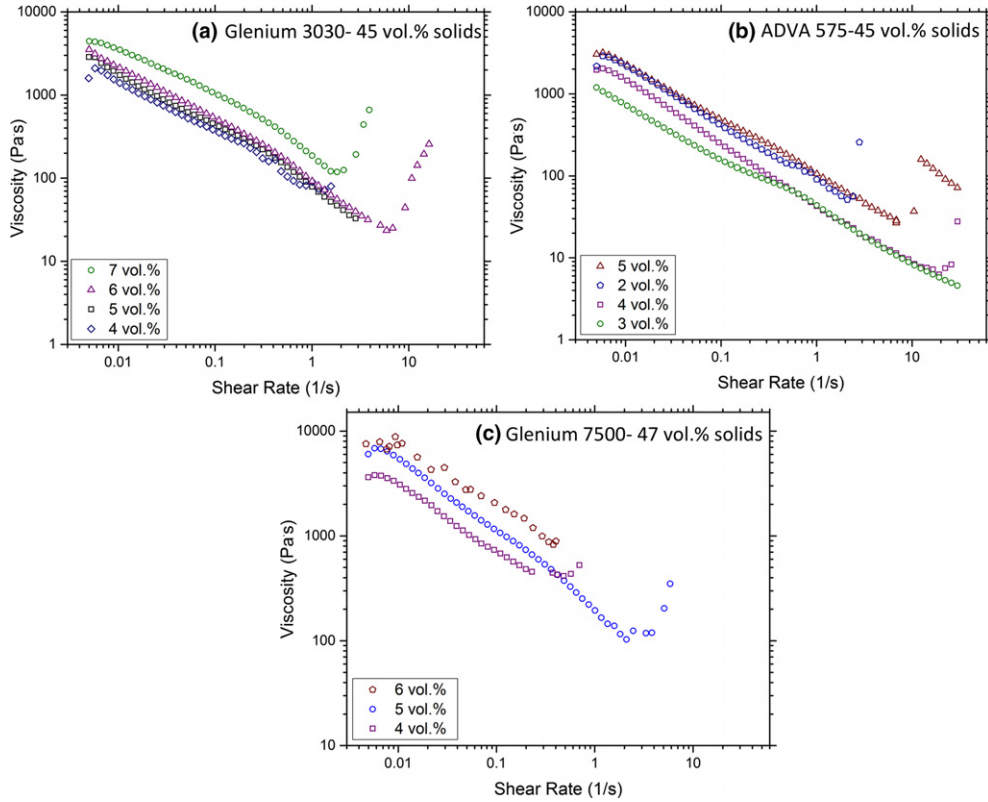


**Fig. 8.** Viscosity as a function of shear rate for suspensions with 45 vol% solids loading and varying dispersant content for (a) Glenium 3030 and (b) ADVA 575. Optimization for (c) Glenium 7500 was done with 47 vol% solids loading in order to see the critical shear rate in the shear rates studied. The optimal dispersant content is chosen as the suspension with the largest critical shear rate.

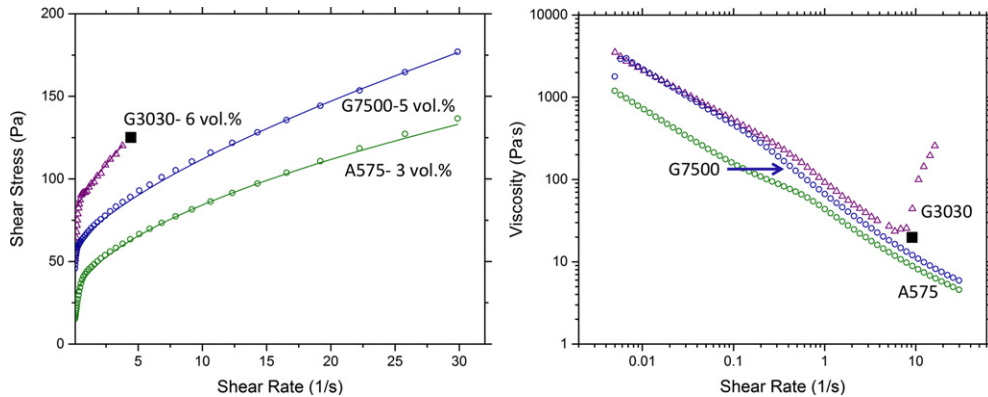


**Fig. 9.** Flow curves for silicon nitride suspensions with 45 vol% solids loading and optimized dispersant amounts for the three studied dispersants. Curve fits to the Herschel–Bulkley fluid model are shown as solid lines with  $R^2 > 0.99$ . The critical shear stress is marked with a (■) for the G3030 sample, the only sample of the three exhibiting shear-thickening behavior. Viscosity as a function of shear rate also shows the G3030 sample has the highest viscosity, followed by G7500 and A575.

likely attributed to inadequate coverage of the ceramic powder.

The rheological curves of the optimum suspensions for each dispersant, based on the experiments outlined in Fig. 8, are plotted together in Fig. 9, with fit parameters listed in Table I. Suspensions made with Glenium 3030 still experienced a critical shear-thickening conversion, while both Glenium 7500 and ADVA 575 remained shear thinning for all shear rates explored. The ADVA 575 sample had the lowest yield stress and viscosity, indicating that it is the most stable and least flocculated suspension of those studied. Both of these samples, though, had low yield stress (less than 55 Pa for both) and viscosities in the range of 75–8 Pa·s at the shear rates of 1–30  $s^{-1}$ , indicating their feasibility as dispersants in this silicon nitride system for low pressure processing.

Shear-thickening behavior is time independent (reversible), so it does not necessarily indicate thixotropic (time-dependent rheology) behavior in a system.<sup>25</sup> If the weak particle flocs in the system, which are broken up upon yielding in a yield-pseudoplastic material, take a longer period of time to reconstruct, the system may exhibit thixotropic behavior.<sup>42</sup> Thixotropic behavior is generally considered undesirable for ceramic forming as the viscosity could change over time causing a formed part to slump. Figure 10 shows viscosity profiles for the two most optimum dispersants (i.e., no shear-thickening behavior during the shear rates studied) at 45 vol % solids loading: Glenium 7500 and ADVA 575. The filled circles are measurements taken at increasing shear rates, while the open circles correspond to immediate decreasing shear rates. The area inside this viscosity hysteresis loop is indicative of the amount of thixotropic behavior of the

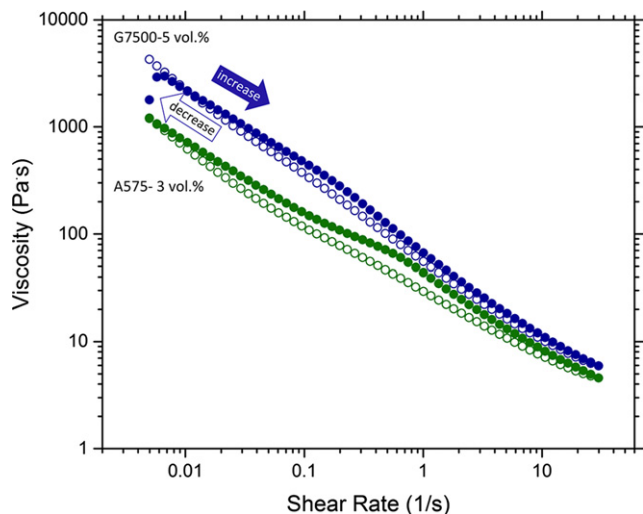


**Fig. 10.** Viscosity as a function of applied increasing, followed by immediate decreasing, shear rate for optimized 45 vol% suspensions using both Glenium 7500 and ADVA 575 as dispersants. G7500 shows little to no thixotropic behavior due to the small gap between viscosity for increasing and decreasing shear rates, while A575 shows a larger gap and therefore slightly more thixotropic behavior.

system. The resultant loops are quite narrow but indicate a small amount of thixotropic behavior of the suspensions, with the ADVA 575 showing a slightly larger loop area and therefore greater level of thixotropy. These small hysteresis loops are expected to have minimal to no impact on ceramic forming at these shear rates due to the low magnitude change in viscosity.

#### IV. Summary

A novel approach of using commercially available concrete comb polymer superplasticizers, called WRAs, was investigated as a means to stabilize highly loaded silicon nitride aqueous suspensions. Four commercially available WRAs were characterized to understand their performance as dispersants in the silicon nitride system. The WRAs with the lowest PAA-Na (backbone) to PEO (side chain) FTIR peak ratio, ADVA 575 and Glenium 7500, performed the best as dispersants at high solids loading (45 vol%) and experienced no shear-thickening behavior at shear rates less than  $30 \text{ s}^{-1}$ . The amount of polymer was optimized to limit shear-thickening behavior with a series of rheological experiments, and 3 vol% ( $1.9 \text{ mg/m}^2$ ) and 5 vol% ( $2.9 \text{ mg/m}^2$ ) of comb polymer dispersant were found to produce optimal suspensions for ADVA 575 and Glenium 7500, respectively. These suspensions exhibit minimal thixotropy and viscosities less than  $75 \text{ Pa}\cdot\text{s}$ , indicating their feasibility for use in low-pressure ceramic-forming processes such as injection molding and additive manufacturing.

#### Acknowledgments

This work was supported by the National Science Foundation Graduate Student Fellowship (Grant DGE-1333468) and by the Army Research Office (Grant W911NF-13-1-042). The authors also thank Professor Carlos Martinez for the rheometer use and training.

#### References

- <sup>1</sup>F. L. Riley, "Silicon Nitride and Related Materials," *J. Am. Ceram. Soc.*, **83** [2] 245–65 (2000).
- <sup>2</sup>S. Hampshire and M. J. Pomeroy, "Grain Boundary Glasses in Silicon Nitride: A Review of Chemistry, Properties and Crystallisation," *J. Eur. Ceram. Soc.*, **32** [9] 1925–32 (2012).
- <sup>3</sup>R. W. Trice and J. W. Halloran, "Mode I Fracture Toughness of a Small-Grained Silicon Nitride: Orientation, Temperature, and Crack Length Effects," *J. Am. Ceram. Soc.*, **82** [10] 2633–40 (1999).

- <sup>4</sup>X. Zhu and Y. Sakka, "Textured Silicon Nitride: Processing and Anisotropic Properties," *Sci. Technol. Adv. Mater.*, **9** [3] 1–47 (2008).
- <sup>5</sup>M. K. Ferber and M. G. Jenkins, "Evaluation of the Strength and Creep-Fatigue Behavior of Hot Isostatically Pressed Silicon Nitride," *J. Am. Ceram. Soc.*, **75** [9] 2453–62 (1992).
- <sup>6</sup>M. A. Janney, O. O. Omatete, C. A. Walls, S. D. Nunn, R. J. Ogle, and G. Westmoreland, "Development of Low-Toxicity Gelcasting Systems," *J. Am. Ceram. Soc.*, **81** [3] 581–91 (1998).
- <sup>7</sup>J. Lenz, R. K. Enneti, S.-J. Park, and S. V. Atre, "Powder Injection Molding Process Design for UAV Engine Components Using Nanoscale Silicon Nitride Powders," *Ceram. Int.*, **40** [1] 893–900 (2014).
- <sup>8</sup>J. Woodthorpe, M. J. Edirisinghe, and J. R. G. Evans, "Properties of Ceramic Injection Moulding Formulations. Part 3 Polymer Removal," *J. Mater. Sci.*, **24**, 1038–48 (1989).
- <sup>9</sup>L. M. Rueschhoff, M. J. Michie, W. J. Costakis, J. P. Youngblood, and R. W. Trice, "Additive Manufacturing of Dense Ceramic Parts via Direct Ink Writing of Aqueous Alumina Suspensions," *Int. J. Appl. Ceram. Technol.*, (in press), doi:10.1111/ijac.12557 (2016).
- <sup>10</sup>V. L. Wiesner, J. P. Youngblood, and R. W. Trice, "Room-Temperature Injection Molding of Aqueous Alumina-Polyvinylpyrrolidone Suspensions," *J. Eur. Ceram. Soc.*, **34** [2] 453–63 (2014).
- <sup>11</sup>V. L. Wiesner, L. M. Rueschhoff, A. I. Diaz-Cano, R. W. Trice, and J. P. Youngblood, "Producing Dense Zirconium Dioxide Components by Room-Temperature Injection Molding of Aqueous Ceramic Suspensions," *Ceram. Int.*, **42** [2] 2750–60 (2016).
- <sup>12</sup>K. Okada, K. Fukuyama, and Y. Kameshima, "Surface-Oxidized Phase in Silicon Nitride and Silicon Oxynitride Powders by X-ray Photoelectron Spectroscopy," *J. Am. Ceram. Soc.*, **78** [8] 2021–6 (1995).
- <sup>13</sup>D. R. Messier, F. L. Riley, and R. J. Brook, "The  $\alpha/\beta$  Silicon Nitride Phase Transformation," *J. Mater. Sci.*, **13** [6] 1199–205 (1978).
- <sup>14</sup>L. Bergstrom and E. V. A. Bostedt, "Surface Chemistry of Silicon Nitride Powders: Electrokinetic Behaviour and ESCA Studies," *Colloids Surf.*, **49** [1] 183–97 (1990).
- <sup>15</sup>S. G. Malghan, "Dispersion of  $\text{Si}_3\text{N}_4$  Powders. Surface Chemical Interactions in Aqueous Media," *Colloids Surf.*, **62** [1–2] 87–99 (1992).
- <sup>16</sup>J. Yang, F. Oliveira, R. Silva, and J. M. Ferreira, "Pressureless Sinterability of Slip Cast Silicon Nitride Bodies Prepared From Coprecipitation-Coated Powders," *J. Eur. Ceram. Soc.*, **19** [4] 433–9 (1999).
- <sup>17</sup>M. I. L. Oliveira, K. Chen, and J. M. Ferreira, "Influence of Powder pre-Treatments on Dispersion Ability of Aqueous Silicon Nitride-Based Suspensions," *J. Eur. Ceram. Soc.*, **21** [13] 2413–21 (2001).
- <sup>18</sup>M. P. Albano and L. B. Garrido, "Processing of Concentrated Aqueous Silicon Nitride Slips by Slip Casting," *J. Am. Ceram. Soc.*, **81** [4] 837–44 (1998).
- <sup>19</sup>S. Hampshire and M. J. Pomeroy, "Silicon Nitride – Grain Boundary Oxynitride Glass Interfaces: Deductions From Glass Bulk Properties," *Int. J. Appl. Ceram. Technol.*, **10** [5] 747–55 (2013).
- <sup>20</sup>J. A. Lewis, "Colloidal Processing of Ceramics," *J. Am. Ceram. Soc.*, **83** [10] 2341–59 (2000).
- <sup>21</sup>A. Kauppi, K. M. Andersson, and L. Bergström, "Probing the Effect of Superplasticizer Adsorption on the Surface Forces Using the Colloidal Probe AFM Technique," *Cem. Concr. Res.*, **35** [1] 133–40 (2005).
- <sup>22</sup>E. Laarz, A. Kauppi, K. M. Andersson, A. M. Kjeldsen, and L. Bergstrom, "Dispersing Multi-Component and Unstable Powders in Aqueous Media Using Comb-Type Anionic Polymers," *J. Am. Ceram. Soc.*, **89** [6] 1847–52 (2006).
- <sup>23</sup>G. H. Kirby and J. A. Lewis, "Comb Polymer Architecture Effects on the Rheological Property Evolution of Concentrated Cement Suspensions," *J. Am. Ceram. Soc.*, **87** [9] 1643–52 (2004).
- <sup>24</sup>D. Lootens, P. Hébraud, E. Lécolier, and H. Van Damme, "Gelation, Shear-Thinning and Shear-Thickening in Cement Slurries," *Oil Gas Sci. Technol.*, **59** [1] 31–40 (2004).
- <sup>25</sup>D. Feys, R. Verhoeven, and G. De Schutter, "Why is Fresh Self-Compacting Concrete Shear Thickening?" *Cem. Concr. Res.*, **39** [6] 510–23 (2009).
- <sup>26</sup>K. Yoshioka, E. Sakai, M. Daimon, and A. Kitahara, "Role of Steric Hindrance in the Performance of Superplasticizers for Concrete," *J. Am. Ceram. Soc.*, **80** [10] 2667–71 (1997).
- <sup>27</sup>C. P. Whitby, P. J. Scales, F. Grieser, T. W. Healy, G. Kirby, et al., "PAA/PEO Comb Polymer Effects on Rheological Properties and Interparticle Forces in Aqueous Silica Suspensions," *J. Colloid Interface Sci.*, **262** [1] 274–81 (2003).
- <sup>28</sup>E. Laarz and L. Bergstrom, "The Effect of Anionic Polyelectrolytes on the Properties of Aqueous Silicon Nitride Suspensions," *J. Eur. Ceram. Soc.*, **20** [4] 431–40 (2000).
- <sup>29</sup>W. Herschel and R. Bulkley, "Consistency of Measurements in Rubber-Benzene Solutions," *Colloid J.*, **39** [19] 291–300 (1926).
- <sup>30</sup>T. F. Tadros, *Rheology of Dispersions: Principles and Applications*, 1st edition. Wiley-VCH Verlag GmbH & Co. KGaA, Weinheim, Germany, 2010.
- <sup>31</sup>M. J. Edirisinghe, M. S. Heidi, and K. L. Tomkins, "Flow Behaviour of Ceramic Injection Moulding Suspensions," *Ceram. Int.*, **18** [3] 193–200 (1992).
- <sup>32</sup>D. Liu and S. G. Malghan, "Role of Polyacrylate in Modifying Interfacial Properties and Stability of Silicon Nitride Particles in Aqueous Suspensions," *Colloids Surfaces A Physicochem. Eng. Asp.*, **110** [1] 37–45 (1996).
- <sup>33</sup>R. Moreno, A. Salomoni, and S. Mello Castanho, "Colloidal Filtration of Silicon Nitride Aqueous Slips. Part I: Optimization of the Slip Parameters," *J. Eur. Ceram. Soc.*, **18** [4] 405–16 (1998).
- <sup>34</sup>L. R. Murray and K. A. Erk, "Jamming Rheology of Model Cementitious Suspensions Composed of Comb-Polymer Stabilized Magnesium Oxide Particles," *J. Appl. Polym. Sci.*, **131** [12] 1–11 (2014).

<sup>35</sup>E. Liden, M. Persson, E. Carlstrom, and R. Carlsson, "Electrostatic Adsorption of a Colloidal Sintering Agent on Silicon Nitride Particles," *J. Am. Ceram. Soc.*, **74** [6] 1335–9 (1991).

<sup>36</sup>V. A. Hackley and S. G. Malghan, "The Surface Chemistry of Silicon Nitride Powder in the Presence of Dissolved Ions," *J. Mater. Sci.*, **29** [17] 4420–30 (1994).

<sup>37</sup>V. A. Hackley, U. Pa, B. Kim, and S. G. Malghan, "Aqueous Processing of Sintered Reaction-Bonded Silicon Nitride: I, Dispersion Properties of Silicon Powder," *J. Am. Ceram. Soc.*, **80** [7] 1781–8 (1997).

<sup>38</sup>V. A. Hackley, "Colloidal Processing of Silicon Nitride with Poly (Acrylic Acid): I, Adsorption and Electrostatic Interactions," *J. Am. Ceram. Soc.*, **80** [9] 2315–25 (1997).

<sup>39</sup>J. E. Smay, J. Cesarano, and J. A. Lewis, "Colloidal Inks for Directed Assembly of 3-D Periodic Structures," *Langmuir*, **84** [18] 5429–37 (2002).

<sup>40</sup>R. L. Hoffman, "Explanations for the Cause of Shear Thickening in Concentrated Colloidal Suspensions," *J. Rheol. (N. Y. N. Y.)*, **42** [1] 111–23 (1998).

<sup>41</sup>M. Cyr, C. Legrand, and M. Mouret, "Study of the Shear Thickening Effect of Superplasticizers on the Rheological Behaviour of Cement Pastes Containing or not Mineral Additives," *Cem. Concr. Res.*, **30** [9] 1477–83 (2000).

<sup>42</sup>A. Nagel, G. Petzow, and P. Greil, "Rheology of Aqueous Silicon Nitride Suspensions," *J. Eur. Ceram. Soc.*, **5** [6] 371–8 (1989). □